Journal of Inflammation Research

Dovepress
Taylor & Francis Group

Open Access Full Text Article

ORIGINAL RESEARCH

PI3 as a Common Hub Gene Linking Atopic Dermatitis and Ulcerative Colitis Through Immune Cell Recruitment Mechanisms

Dan Jian, Jian Chen, Jinping Yuan, Kunwar Namrata, Dan Su, Bingxue Bai

Department of Dermatology, The Second Affiliated Hospital of Harbin Medical University, Harbin, 150000, People's Republic of China

Correspondence: Bingxue Bai, Department of Dermatology, The Second Affiliated Hospital of Harbin Medical University, 246 Xuefu Road, Nangang, Harbin, 150000, People's Republic of China, Tel +86-15114517408, Email baibingxue@hrbmu.edu.cn

Background: Atopic dermatitis (AD) and ulcerative colitis (UC) are increasingly prevalent, and growing evidence suggests a potential link between them. However, the shared pathogenesis remains unclear. This study aims to identify the hub genes and immunological features underlying the connection between AD and UC.

Methods: In this study, we downloaded the GSE121212 and GSE75214 datasets from the GEO database. Differentially expressed genes (DEGs) were identified through DESeq2 and limma R packages, revealing enrichment in immune-related pathways such as neutrophil migration and chemokine signaling. Subsequently, weighted gene co-expression network analysis (WGCNA) and protein-protein interaction (PPI) network analysis were performed to identify common candidate genes. Three machine learning algorithms were employed to select the hub gene, and single-cell RNA sequencing was used to validate the findings.

Results: Seven common candidate genes (CXCL1, CCL20, CXCL2, ZC3H12A, PI3, CXCL3, LCN2) were identified, showing significant expression differences in both diseases and associations with immune cell infiltration. Among them, PI3 emerged as the hub gene with strong diagnostic potential (AUC > 0.95) based on three machine learning models. Single-cell RNA sequencing supported high PI3 expression in UC intestinal epithelial cells and AD keratinocytes, with correlations to certain CCL and CXCL chemokines. These chemokines play overlapping roles in recruiting M1 macrophages, CD4 T cells, and neutrophils, thereby regulating inflammation in both AD and UC.

Conclusion: Our study uncovers shared immune cell recruitment mechanisms in both diseases, suggesting that CCR1 may serve as a potential common target. Additionally, PI3 is identified as a potential biomarker for both AD and UC, providing new insights into the mechanisms and potential connections between these diseases.

Keywords: biomarkers, machine learning, immune recruitment, single-cell RNA sequencing, neutrophil

Introduction

Atopic dermatitis (AD) is a prevalent inflammatory skin disorder characterized by eczema-like lesions, intense pruritus, and a recurrent course.[1] Its prevalence has increased in recent years, affecting approximately 20% of children and 7–14% of adults, leading to substantial socio-economic burdens.[2] Emerging evidence suggests that AD may be a systemic inflammatory disease associated with inflammatory comorbidities, including inflammatory bowel disease (IBD).[3]

Ulcerative colitis (UC), a subtype of IBD, is distinguished by chronic intestinal inflammation, presenting with symptoms such as bloody diarrhea, abdominal pain, and tenesmus.[4] Over the past decade, UC has emerged as a global public health imperative.[5] Notably, UC extends beyond the digestive system, affecting cutaneous tissues and showing a strong correlation with AD.[6]

Recent investigations have revealed a bidirectional association between AD and UC.[7,8] In particular, adult patients with AD show a significantly increased risk of developing UC.[9,10] It has been documented that both AD and UC are ailments that involve a compromised superficial barrier. Barrier defects may result in a pathological condition

Received: 11 March 2025
Accepted: 26 June 2025
Published: 27 August 2025

characterized by the colonization of opportunistic bacteria and migration of immune cells, thereby instigating enhanced local inflammation and disruption of the barrier at distant sites.[11,12]

Indeed, AD and UC share common immunological features, including Th2 cell dominance during the acute phase of AD and the involvement of Th1, Th17, and Th22 cells during the chronic phase. Similarly, UC is primarily driven by Th2-type inflammation but also involves Th1 and Th17 responses.[12–14] In addition, AD and UC share multiple susceptibility loci that encompass genes pertinent to adaptive immunity, including STAT3, CCL17, CCR4, and IL2/IL2.[3,15] Despite advancements in the field, the specific immune cells and associated cytokines engaged in this mechanism remain unclear, and there is a deficiency of reliable biomarkers capable of prognosticating the concurrent manifestation of AD and UC.

To date, there is a lack of systematic studies integrating bulk and single-cell transcriptomic analyses to explore the shared pathogenic mechanisms between AD and UC. This study aims to predict potential biomarkers and common pathways of AD and UC by integrating both data types, thereby elucidating their pathogenesis from an immunological perspective.

Methods

Data Preprocessing and Differential Expression

Samples were acquired from the gene expression omnibus (GEO) database (http://www.ncbi.nlm.nih.gov/geo/). The series matrix files of GSE121212 and GSE75214 were subjected to be data preprocessed separately. Subsequently, we employed |FC|>2 and p-adjust<0.05 as the filtration conditions using the "DESeq2" R package and "limma" R package to isolate the differentially expressed genes (DEGs) in the two datasets independently.[16] The R package "ggplot" was deployed to map the differentially expressed genes of DEGs procured from the two datasets.

Enrichment Analysis Analysis

The enrichment analyses of DEGs were executed by the clusterProfiler package.[17] Gene ontology (GO) is primarily concerned with specific functional classifications of genes,[18] and encyclopedia of genes and genomes (KEGG) is chiefly engaged in the gene-associated signaling pathways.[19–21] The regulation and function of genes across various biological conditions were evaluated using Gene Set Enrichment Analysis (GSEA).

Weighted Gene Co-Expression Network Analysis (WGCNA)

WGCNA is a computational methodology to explore the associations between co-expressed genes and disease phenotypes.[22] Initially, the co-expression matrix for top 75% of genes filtered by median absolute deviation (MAD) screened was determined by calculating the Pearson correlation coefficients. Based on the calculated soft threshold β, the topology matrix TOM, the hierarchical clustering tree and gene modules are successively generated. Modules were selected based on their clinical characteristics demonstrating highest correlation coefficients, and p-values of <0.05 were considered. The genes in these modules and up-DEGs were intersected by constructing Venn diagrams through the online jvenn website (http://jvenn.toulouse.inra.fr/app/example.html), which served as the subsequent step in the analysis.

PPI (Protein-Protein Interaction) Network and Expression Validation

The STRING database (https://string-db.org/) and cytoscape software was utilized for PPI network fabrication.[23] The CytoHubba plugin in Cytoscape was utilized to quantify the magnitude of protein nodes, and edge penetration component (EPC) algorithms were selected to identify candidate genes.[24] Subsequently, the receiver operator characteristic (ROC) curve was plotted, and the diagnostic utility of reliable candidate genes was evaluated by calculating the area under the ROC (AUC). An AUC>0.8 was considered indicative of ideal diagnostic value. Moreover, GSE16161 and GSE87466, as external validation cohorts, were employed for verification of candidate gene expression levels.

Immune Analysis Algorithm

CIBERSORT is a prevailing method for calculating immune cell infiltration, which employs the principle of linear support vector regression to deconvolve the expression matrix of 22 immune cell subtypes to estimate the abundance of

immune cells.[25] In R software, the correlation between candidate biomarkers and immune-infiltrated cells was determined by Spearman rank correlation analysis, and the result visualization was rendered by the "ggplot2" package.

Machine Learning Analysis

To further screen for diagnostic hub genes, three machine learning algorithms were applied. The least absolute shrinkage and selection operator (LASSO) is a regression analysis algorithm that discards genes with minimal contribution to the disease via the "glmnet" package, thereby isolating those of greater significance.[26] The Random Forest method, utilizing the "randomforest" package, was applied to assess and rank the relative importance of each gene.[27] Additionally, support vector machine - recursive feature elimination (SVM-RFE) is an embedded-based machine analysis algorithm that sieves the optimal features of the data.[28] The "e1071 R" package is employed to execute the SVM classifier model.

miRNA-TF-mRNA Network Construction

The human microRNA disease database (HMDD) was utilized to identify common miRNAs associated with both AD and UC diseases.[29] Subsequently, the TransmiR database was employed to procure the TFs of these miRNAs.[30] Concomitantly, TFs targeting the hub genes were predicted using the PROMO database, and the resulting regulatory network was visualized using Cytoscape.[31] Promoter sequences of these hub genes were retrieved from the NCBI database. Ultimately, the shared miRNAs, hub genes, and transcription factors were integrated to construct a miRNA–TF–mRNA regulatory network using Origin software.

Immunohistochemistry (IHC)

IHC was utilized to assess the relative protein expression levels of pivotal markers in patients with AD and UC, respectively. The samples required for this study were obtained from May 2023 to December 2023 at the Department of Dermatology of the Second Affiliated Hospital of Harbin Medical University and the Department of Pathology of the Second Affiliated Hospital of Harbin Medical University. The sample consisted of 12 lesional skin tissues from patients with moderate-to-severe AD and 5 normal human skin tissues, and 8 active UC intestinal lesions and 5 normal human intestinal tissues. All samples were confirmed by pathologists and dermatologists to be AD, UC and normal human tissues.

Single-Cell RNA Sequencing (scRNA-Seq) Analysis

ScRNA-seq data were obtained from GSE214695 (6 UC and 6 HC biopsy samples), GSE197023 (3 AD and 2 HC suction blister samples) and GSE153760 (3 AD and 4 HC biopsy samples), which were processed utilizing the "Seurat" package in R. To ensure data quality, we removed doublets, filtered out cells with more than 10% mitochondrial gene content, and corrected for batch effects using the "harmony" package. The Uniform Manifold Approximation and Projection (UMAP) algorithm was employed for cell clustering, with each cluster being annotated through a combination of literature review and the "SingleR" package. Finally, we utilized the "CellChat" package to calculate ligand-receptor interactions and construct the cell communication network.

Results

The Data Information and Expression of Differential Gene

The data sets for the AD dataset GSE121212 and the UC dataset GSE75214 were incorporated into this study (Table 1). Through difference analysis, the AD dataset comprised 1751 up-regulated expression of differential genes (DEGs) and 1500 down-regulated DEGs. The UC dataset encompassed 660 up-regulated DEGs and 494 down-regulated DEGs. A total of 136 genes manifested overlap in the up-regulated genes of AD and UC, while 43 genes were found to be co-down-regulated (Figure 1A).

Table 1 Summary of Those Four GEO Datasets Involving AD and UC Patients

Data Set	Samples	Tissue	Disease	Group
GSE140684	21 from lesions skin and 38 from healthy skin	Skin	AD	Discovery cohort
GSE75214	97 form UC and 22 from controls	Colon and ileum	UC	Discovery cohort
GSE16161	9 from lesional skin and 9 from healthy skin	Skin	AD	Validation cohort
GSE87466	87 form UC and 21 from controls	Colon	UC	Validation cohort
GSE214695	6 UC and 6 HC biopsy samples	Colon	UC	ScRNA-seq
GSE197023	3 AD and 2 HC samples	Skin	AD	ScRNA-seq
GSE153760	3 AD and 4 HC biopsy samples	Skin	AD	ScRNA-seq

Abbreviations: AD, atopic dermatitis; UC, ulcerative colitis; scRNA-seq, single-cell RNA sequencing.

Functional Enrichment Analysis

For co-up-regulated genes, KEGG pathway was enriched in cytokine-cytokine receptor interactions, JAK-STAT signaling pathways and other immune and inflammation-associated pathways, whereas the co-down-regulated genes were primarily associated with metabolic pathways (Figure 1B). The peaks plot of GSEA indicated that the genes were upregulated in monocytes or dendritic cells within specific immune-related gene sets (Figure 1C). According to the chord plot, GO enrichment was predominantly enriched in leukocyte migration, response to lipopolysaccharide, and neutrophil migration (Figure 1D).

Identification of Disease-Related Key Modules

In the UC dataset, one outlier was eliminated, and the optimal soft threshold was ascertained to be 16 by the "WGCNA" package. Parameters such as minModuleSize=100, deepSplit=2, and MEDissThres=0.25 were established as the clustering conditions, and 15 modules were identified. The magenta module ($R=0.64$ and $P<0.05$), comprising 555 genes, had the highest correlation with AD (Figure 2A–C). With the same methodology, 10 modules were again discerned in the AD dataset, applying a soft threshold of 16. The tan module ($R=0.85$ and $P<0.05$) was selected as having the highest correlation with AD, comprising 2019 genes (Figure 2D–F).

Identification and Validation of Candidate Genes

By intersecting the up-regulated genes and positively correlated modules of AD and UC, we obtained a more central set of 26 genes (Figure 3A). Subsequently, we undertook PPI network analyses to quantify and rank the core importance of the genes (Figure 3B). Ultimately, 7 common candidate genes were ascertained, comprising CXCL1, CCL20, CXCL2, ZC3H12A, PI3, CXCL3, and LCN2 (Figure 3C). Concomitantly, the AUC values of exceeded 0.8, thereby supporting that they possess favorable diagnostic properties for AD (Figure 3D) and UC (Figure 3E). In external datasets, violin plots demonstrated a significantly elevated expression of candidate genes in AD lesions compared to healthy controls (Figure 3F), as well as in UC tissues relative to healthy controls (Figure 3G). To further elucidate the role of the candidate genes in immune infiltration, we conducted a correlation analysis between the candidate genes and the abundance of immune cells. As anticipated, the seven candidate genes exhibited a strong correlation with immune cell.

Machine Algorithms for Screening Hub Biomarkers

Genes with importance scores exceeding 2 were selected using the random forest algorithm, resulting in four genes for AD (Figure 4A and B). The LASSO algorithm, when minimizing the mean squared error (MSE), identified ZC3H12A and PI3 as being more prominently characterized in AD (Figure 4C). SVM-RFE analysis further confirmed that ZC3H12A and PI3 had the greatest impact on AD (Figure 4D). For UC, the random forest algorithm identified six relevant genes (Figure 4E and F). LASSO regression analysis showed that PI3 and CXCL3 had the strongest predictive power (Figure 4G), while SVM-RFE analysis indicated that all seven candidate genes had significant effects on UC (Figure 4H). Consequently, we identified PI3, a co-overlapping feature gene, as an optimal diagnostic biomarker for both AD and UC (Figure 4I).

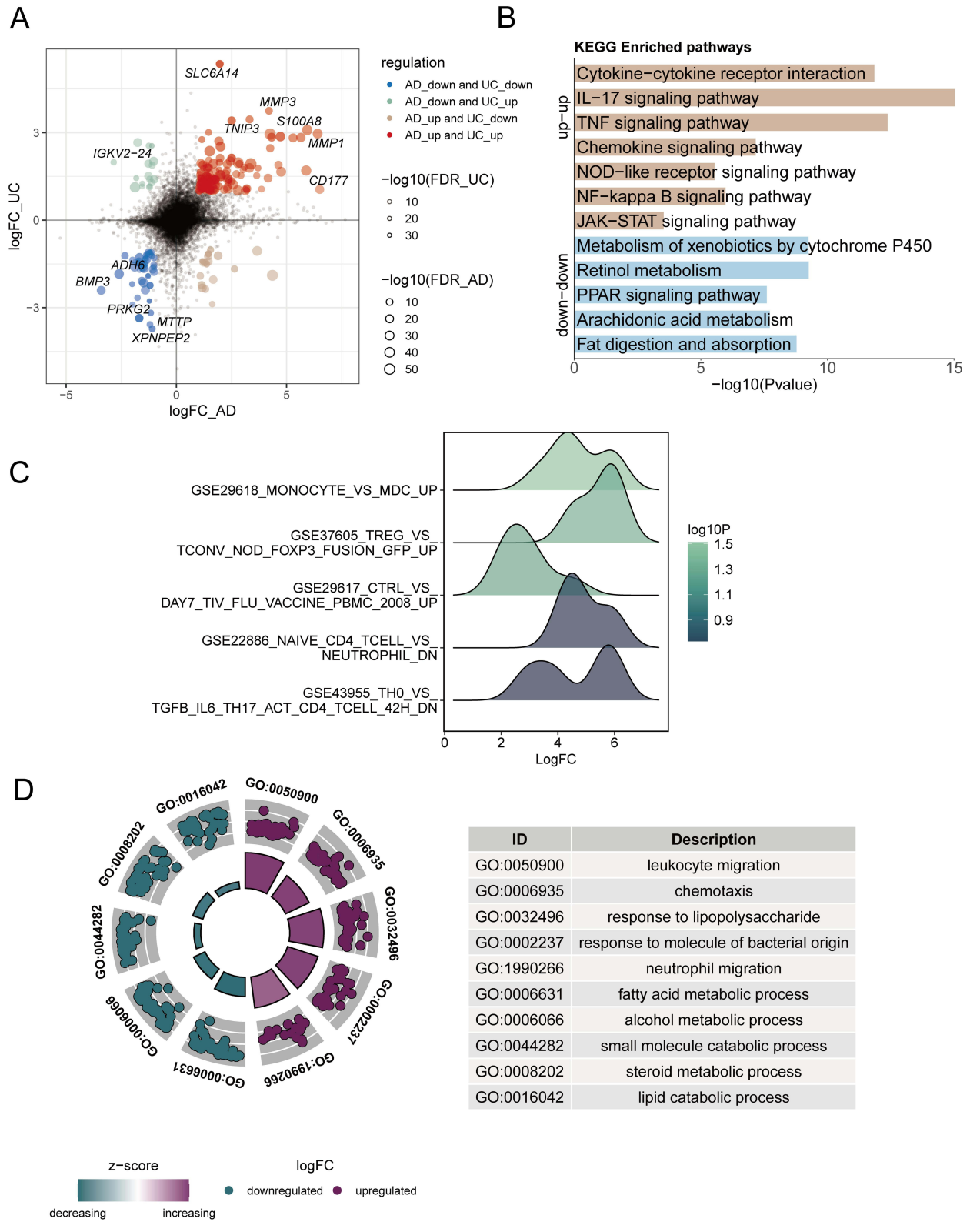

ID	Description
GO:0050900	leukocyte migration
GO:0006935	chemotaxis
GO:0032496	response to lipopolysaccharide
GO:0002237	response to molecule of bacterial origin
GO:1990266	neutrophil migration
GO:0006631	fatty acid metabolic process
GO:0006066	alcohol metabolic process
GO:0044282	small molecule catabolic process
GO:0008202	steroid metabolic process
GO:0016042	lipid catabolic process

Figure 1 Enrichment analysis results of DEGs. (**A**) Overlapping shared genes between the AD and UC. (**B**) The KEGG analysis of DEGs. (**C**) GSEA analysis of DEGs. (**D**) The GO analysis of DEGs.

Abbreviations: DEGs, differentially expressed genes; GO, gene ontology; KEGG, kyoto encyclopedia of genes and genomes; GSEA, gene set enrichment analysis.

https://doi.org/10.2147/JIR.S527507

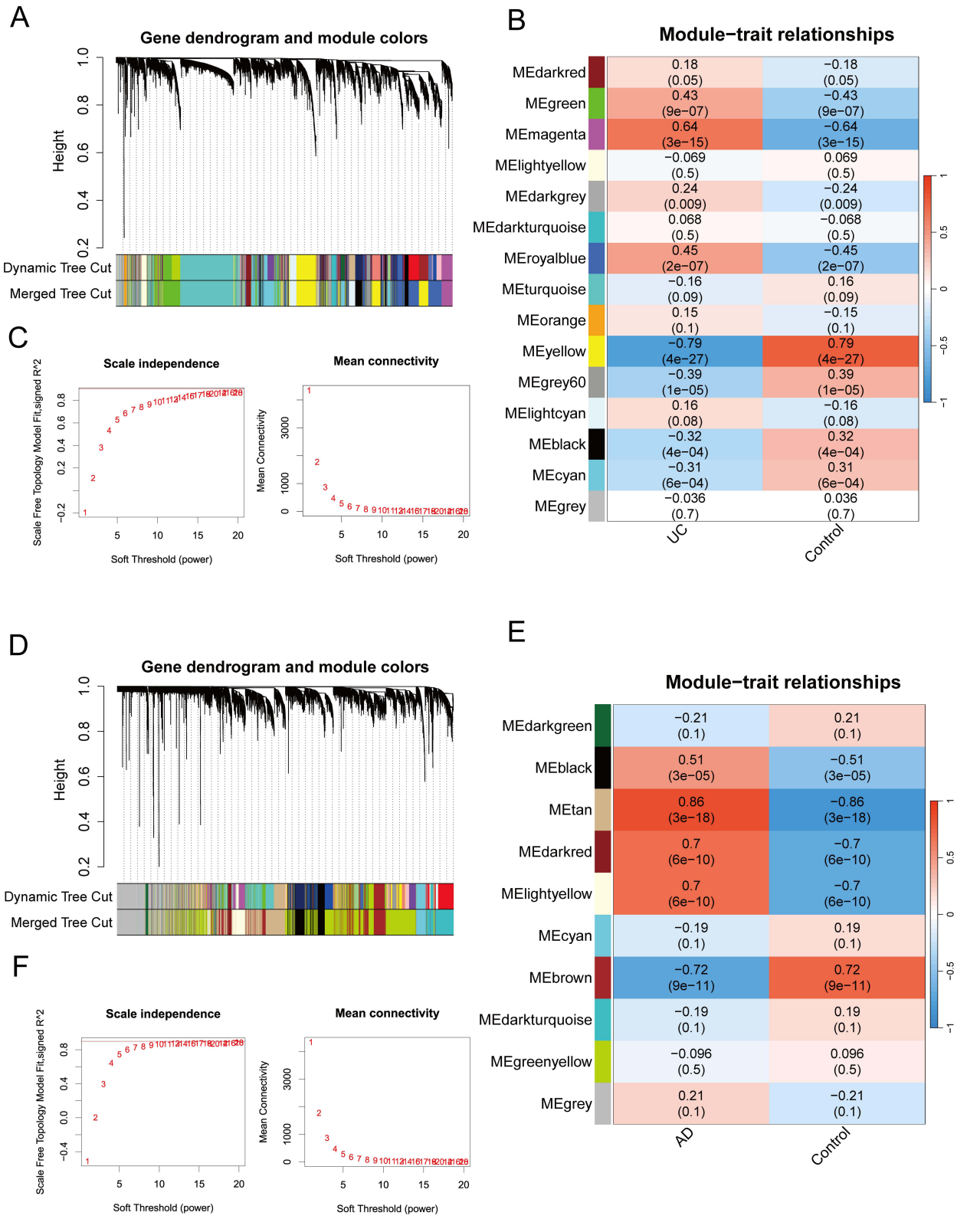

Figure 2 The results from WGCNA. (**A**) The cluster dendrogram of co-expression genes in UC. (**B**) Module–trait relationships in UC, each module contains the corresponding correlation and *p*-value. (**C**) Scaleless index and average connectivity of individual soft thresholds for UC. (**D**)The cluster dendrogram of co-expression genes in AD. (**E**) Module–trait relationships in AD. (**F**) Scaleless index and average connectivity of individual soft thresholds for AD.
Abbreviation: WGCNA, weighted gene co-expression network analysis.

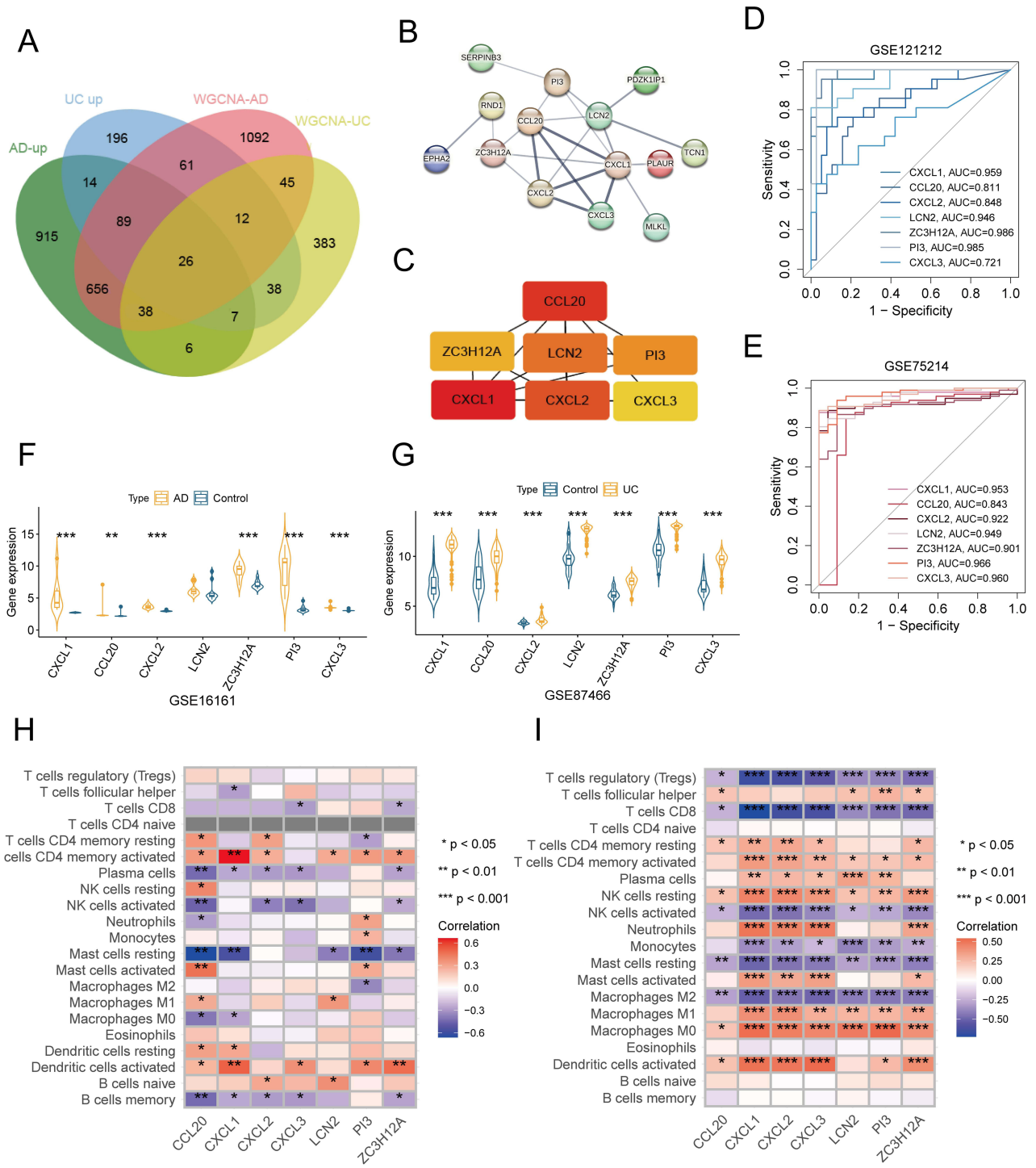

Figure 3 Protein interaction network construction and visualization. (**A**) The Venn diagram showed the intersecting gene between up-DEGs and positively correlated modules. (**B**) PPI network construction. (**C**)Top 7 genes in Cytohubba software by EPC algorithm. (**D**) AUC of the candidate genes in GSE121212. (**E**) AUC of the candidate genes in GSE75214. (**F** and **G**) The expression levels of the candidate genes between disease group(yellow) and normal control group(blue) in the validation cohort (GSE16161 and GSE87466). (**H** and **I**) Correlation matrix of candidate genes and cells calculated by CIBERSORT in AD and UC. *P<0.05, **P<0.01, ***P<0.001.
Abbreviations: EPC, edge penetration component; ROC, receiver operator characteristic; AUC, area under the curve of ROC; PPI, protein–protein interaction.

Construction of miRNA-TF-mRNA Network

Predicated upon the evidence accrued from the HMDD database, 58 miRNAs were isolated in AD, and 35 miRNAs in UC; 16 miRNAs (has-miR-155, has-miR-21, has-miR-223, etc) were ascertained as common miRNAs intersecting both AD and IBD. Thenceforth, interactions between target genes and TFs were prognosticated by PROMO, and 17

https://doi.org/10.2147/JIR.S527507

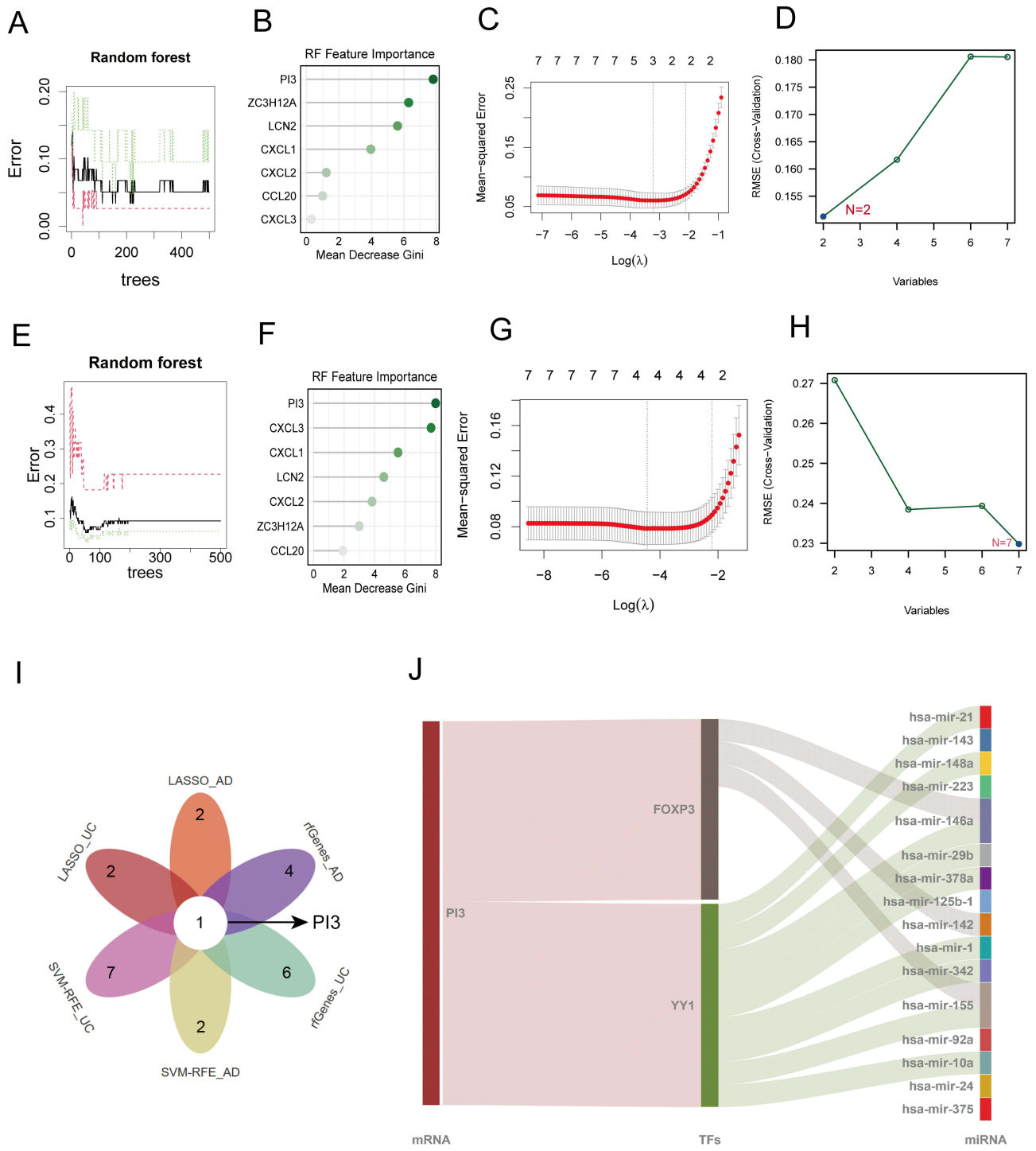

Figure 4 Machine learning and miRNA-TF-mRNA network of the hub gene. (**A** and **B**) The Random Forest algorithm was used to analyze the correlation between the total number of trees in the AD dataset and the error rate, alongside ranking the relative importance scores of genes. (**C**) Optimal Feature Selection Using LASSO for AD. The optimal λ value through cross-validation to ensure model stability. (**D**) In SVM-RFE analysis, the lowest point on the curve signifies the number of genes that significantly contribute to the disease. (**E** and **F**) Random Forest Error Convergence and importance score ranking of genes for UC. (**G**) Optimal Feature Selection Using LASSO for UC. (**H**) SVM-RFE Optimal Variables for UC Classification. (**I**) Intersections are shown in petalogram. (**J**) miRNA-TF-mRNA network of the biomarker construction.
Abbreviations: LASSO, the least absolute shrinkage and selection operator; SVM-RFE, support vector machine - recursive feature elimination.

TFs were uncovered. The interactional network was architected via Cytoscape software, wherein FOXP3 and YY1 could engage with above miRNAs. A visualized alluvial diagram elucidates key mRNA-TF-miRNA molecular regulatory axes (Figure 4J), encompassing has-miR-155/ YY1/PI3, has-miR-142/FOXP3/PI3 etc.

Relative Protein Expression Levels of the Hub Marker

Positive expression of PI3 was predominantly observed within the keratin-forming cells of the epidermal epithelium in AD, accompanied by a minor extracellular expression. The expression of PI3 in AD exhibited a statistically significant disparity when compared to normal skin tissue (p value < 0.0001) (Figure 5A). To assess the diagnostic efficacy of the screened gene, we employed ROC curve analysis. The AUC values of PI3 exceeded 0.95 in AD (Figure 5B). Similarly, in UC, PI3 was detected on the surface of the intestinal mucosa and within the epithelial cells, displaying a significant deviation from normal intestinal tissue (p value < 0.01) (Figure 5C). The AUC value of PI3 also exceeded 0.95 in UC (Figure 5D), supporting its favorable diagnostic potential for both AD and UC.

Single-Cell Characterization and Cellular Communication in UC

To further substantiate the expression patterns of candidate genes, we conducted an analysis of single-cell data from AD and UC samples. Our analysis identified 19,244 cells in AD tissue and 17,219 cells in UC tissue. In the UC dataset, all cells were categorized into six distinct clusters (Figure 6A). Compared to the healthy population, UC patients exhibited an increase in immune cells and a decrease in intestinal epithelial cells (Figure 6B). Subsequently, we evaluated the expression levels of the candidate core genes across different cell clusters (Figure 6C). We further isolated T cells and

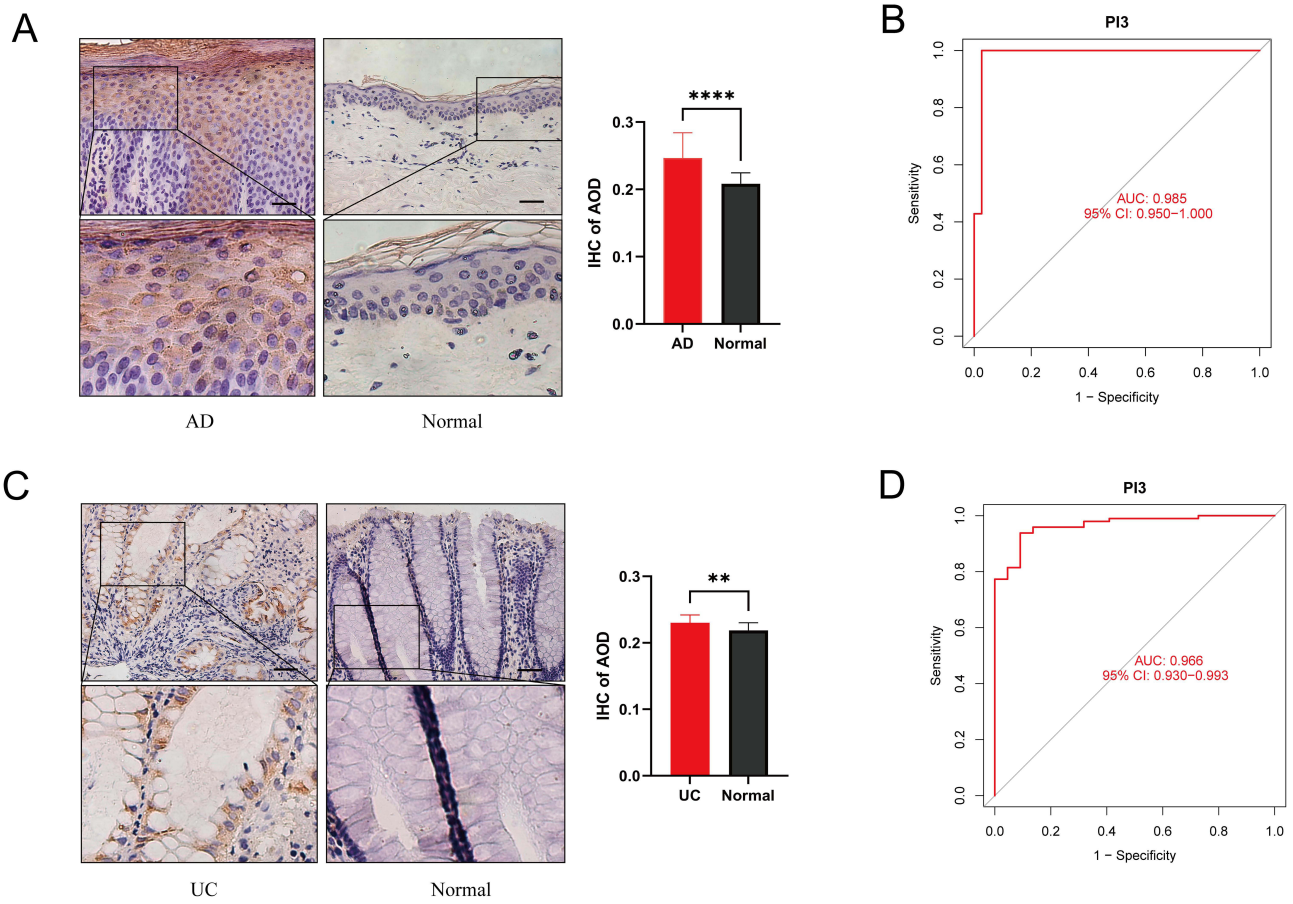

Figure 5 Immunohistochemical analyses of hub gene. (**A**) AD samples showed relatively strong expression of PI3 in keratin-forming cells. (**B**) ROC curve of the three feature genes in the AD discovery cohort. (**C**) UC samples showed relatively strong expression of PI3 in epithelial cells. (**D**) ROC curve of the three feature genes in the UC discovery cohort. **P<0.01, ****P<0.0001, Scale bar = 50 μm.

https://doi.org/10.2147/JIR.S527507

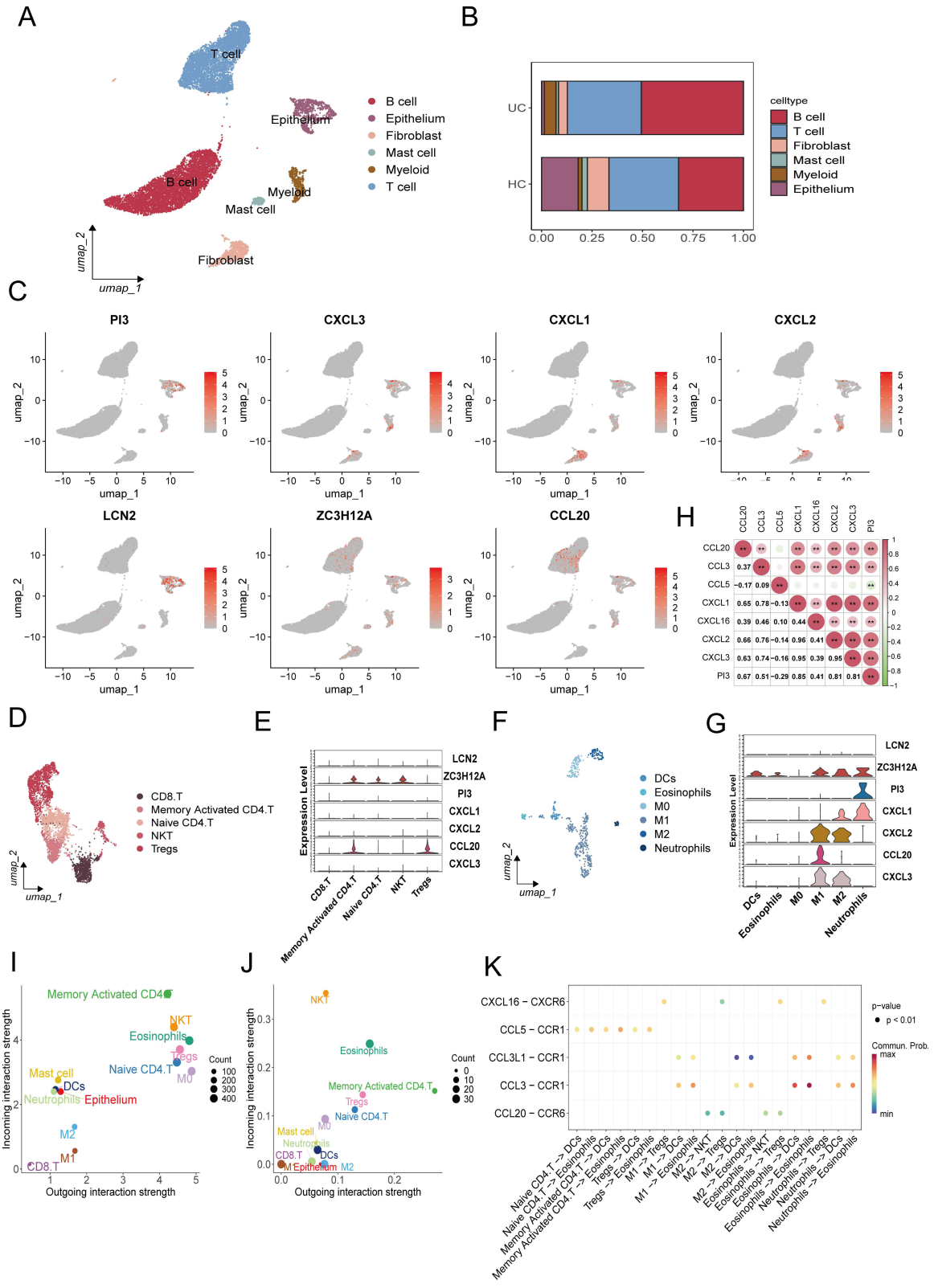

Figure 6 ScRNA-seq analysis of UC and healthy samples. (**A**) UMAP clustering was performed on cells integrated from 6 UC and 6 HC biopsy samples. (**B**) Cell scale graph showing proportional changes in cell populations between HC and UC. (**C**) UMAP diagram showing gene expression patterns in different cell types. (**D**) UMAP Clustering of T Cell subsets. (**E**) Violin plots showing the expression levels of candidate genes across different T cell subtypes. (**F**) UMAP clustering of myeloid cells. (**G**) Violin plots showing the expression distribution of candidate genes across different myeloid cell populations. (**H**) Spearman correlation matrix showing the relationships between PI3 and chemokines. (**I**) Bubble plot quantifying the strength of signaling received by different immune cell subsets. (**J**) Bubble plot illustrating the strength of signaling sent by different immune cell subsets. (**K**) Dot plot showing interactions between the top five chemokines and their receptors among different immune cell subsets. *P<0.05, **P<0.01.
Abbreviations: UMAP, manifold approximation and projection; HC, healthy control; DCs, dendritic cells; M, Macrophages.

myeloid cells, subdividing them into six and three clusters, respectively. PI3 showed high levels of expression in UC intestinal epithelial cells and neutrophils. CCL20 was predominantly expressed in memory-activated $CD4^+$ T cells. CXCL2 and CXCL3 were mainly expressed in M1/M2 macrophages, while CXCL1 was highly expressed in M1 macrophages and neutrophils. ZC3H12A was widely distributed among various cell types (Figure 6D–G). Furthermore, PI3 exhibits significant positive correlations with multiple chemokines, suggesting that it is likely involved in the regulatory network of these chemokines ($P < 0.05$) (Figure 6H).

To elucidate the role of various immune cells in signaling, we conducted an analysis of intercellular communication. Our findings indicate that Memory Activated CD4 T cells, Eosinophils, and NK T cells assume a pivotal regulatory function in signaling within UC (Figure 6I). These cells are capable of both sending and receiving signals within the CCL and CXCL signaling pathways (Figure 6J). The top five contributors to receptor-ligand interactions within the CCL and CXCL signaling pathways, which facilitate information transmission and immune cell activation, included CCL3-CCR1, CXCL13-CCR1, CCL20-CCR6, among others (Figure 6K).

Single-Cell Characterization and Cellular Communication in AD

The AD dataset was systematically categorized into 16 distinct cellular clusters (Figure 7A). Analysis revealed that patients with AD exhibited an increase in immune cell populations and a decrease in epidermal cells relative to healthy individuals (Figure 7B). Notably, the expression levels of PI3 were predominantly elevated in keratinocytes, particularly within the suprabasal layer. The expression levels of CXCL1, CXCL2, CXCL3, and CCL20 were found to be elevated in immune cells, mirroring the expression patterns observed in UC (Figure 7C). Additionally, correlation heatmaps demonstrated significant associations between PI3 and CXCL1, CXCL3, and CCL20 ($P < 0.05$) (Figure 7D). The cellular communication results showed that basal keratinocytes (Basal KC), proliferating keratinocytes (Proliferating KC), plasmacytoid dendritic cells (pDC), and M2 macrophages demonstrated higher intensities of both sending and receiving signals in AD, suggesting their pivotal role in the signaling network (Figure 7E). Based on the transcriptome results, we focused on the chemokine signaling pathway and found that supraspinous KC and proliferating KC exhibited significant sensitivity to CXCL signaling and were identified as principal sources of such signals (Figure 7F). In contrast, T cells and conventional dendritic cells type 1 (cDC1) predominantly acted as the signal recipients, highlighting their crucial role in responding to chemotactic signals. The ligand CCL13 and the receptor CCL3, which significantly contribute to the CCL and CXCL signaling pathways, establish strong interactions with CCR1 and CCR6. The results suggest that AD and UC share similar immune activation profiles, especially involving the recruitment of immune cells such as macrophages, T cells, and neutrophils.

Discussion

In this study, we combined transcriptome sequencing data and single-cell expression profiling to elucidate the shared immunological mechanisms underlying AD and UC and to identify potential biomarkers. Firstly, we isolated 26 common DEGs by difference analysis and WGCNA using datasets from the GEO database. The enrichment analyse results suggested abnormal migration of neutrophils, cytokine-cytokine receptor interactions, and JAK-STAT signaling pathways may be implicated in both diseases. Subsequently, we constructed a PPI network to screen seven candidate genes (CXCL1, CCL20, CXCL2, ZC3H12A, PI3, CXCL3, LCN2) and verified their high expression levels and diagnostic utility using external datasets. In addition, three machine learning algorithms were used to apply the identification of a hub gene (PI3), and external datasets supported its strong diagnostic performance (ROC>0.95). Immunohistochemical (IHC) validation confirmed its high level of expression in both AD and UC. Notably, we employed single-cell RNA sequencing (scRNA-seq) to assess the expression of key genes in cells and further investigated chemokine interactions between these cells. Our findings indicate that PI3 has the potential to serve as a diagnostic biomarker for AD and UC, as well as that CCL and CXCL signaling molecules emerge as potential targets for modulating immune responses in both diseases.

PI3, also known as SKALP or elafin, is a specific protease inhibitor that functions to inhibit tissue protein degradation and inflammation induced by neutrophil elastase and elastase 2a (ELA2A). Our analysis revealed elevated expression of PI3 in both adult AD lesional skin and UC intestinal epithelium. Notably, it was learned that increased PI3 expression

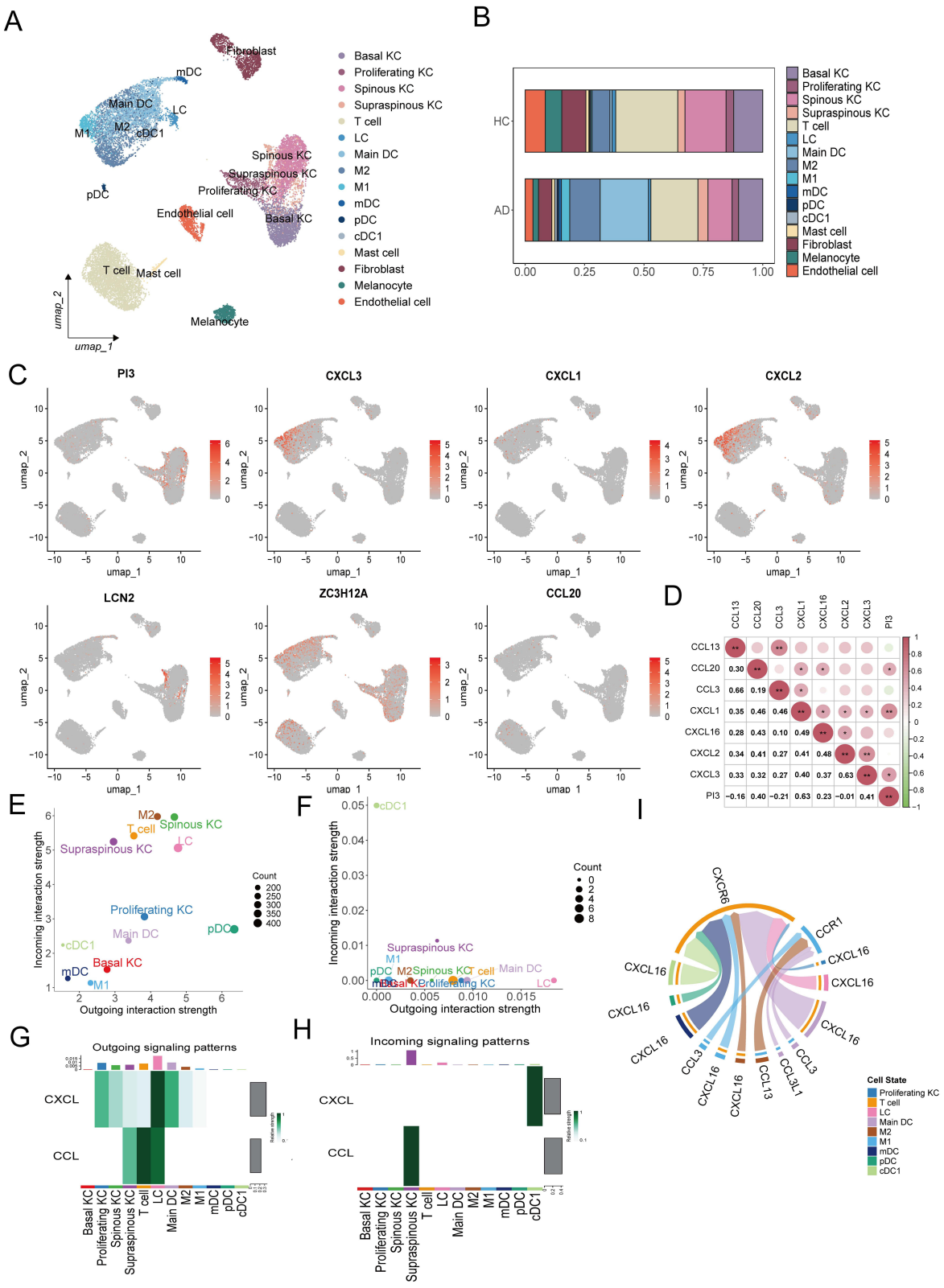

Figure 7 ScRNA-seq analysis of AD and healthy samples. (**A**) UMAP clustering was performed on cells integrated from healthy skin (n = 4), AD lesion skin (n = 3), and AD (n = 3) suction blister and HC (n = 2) suction blister samples. (**B**) Proportional changes in cell populations between HC and AD. (**C**) Expression patterns of candidate genes across different cell populations. (**D**) Spearman correlation matrix showing the relationships between PI3 and chemokines. (**E**) Global signaling interaction strengths among different cell types. (**F**) CXCL and CCL signaling interaction strengths. (**G**) Outgoing signaling patterns of CXCL and CCL chemokine families. (**H**) Incoming signaling patterns of CXCL and CCL chemokine families. (**I**) A circle plot illustrated the top five ligand-receptor interactions related to CXCL and CCL. *P<0.05, **P<0.01.
Abbreviations: KC, keratinocyte; LC, langerhans cell; mDC, myeloid dendritic cell; pDC, plasmacytoid dendritic cell; cDC1, conventional dendritic cell 1.

found exclusively in UC among the two subtypes of IBD, highlighting its specificity in UC and suggesting its potential as a diagnostic marker to differentiate between CD and UC phenotypes.[32] Some researchers have found that serum PI3 levels correlate with AD severity, and that there was a significant positive correlation between lesional/non-lesional skin and blood expression of PI3.[33] This correlation revealed a possible inflammatory amplification of AD.

Significantly, through single-cell mapping and IHC, we determined that PI3 exhibited heightened expression in keratinocytes of AD skin lesions and epithelial cells of UC. This elevated expression may be attributed to PI3's known role in enhancing the epithelial barrier and its antimicrobial properties.[34] The aforementioned findings suggest that PI3 has the potential to serve as a common biomarker for AD and UC.

Our study further highlights that CCL and CXCL signaling molecules have common targets of action in both AD and UC. CCL20, CCL3 chemokines play a crucial role in the recruitment of macrophages, dendritic cells, CD4 T cells, and eosinophils, which primarily regulate chronic inflammation, while CXCL1/2/3 chemokines mainly regulate neutrophil migration. These findings align with our results. Specifically, CCL3/CCL3L1-CCR1 and CXCL13/CXCL16-CCR1 were found to have pro-inflammatory roles in both UC and AD immune environments. This suggests that AD and UC may share similar immune activation patterns, which may influence disease progression or even contribute to the development of comorbidities.

On the basis of the immunoassay results, the upregulation of PI3 was found to be associated with increased abundance of memory activated CD4 T, plasma cells, and neutrophils. This may be attributed to two factors: on the one hand, PI3 likely plays a role in the activation or proliferation of these immune cells, and on the other hand, PI3 was positively correlated with the expression of chemokines such as CXCL1, CXCL3, and CCL20, whose elevated levels may promote the recruitment of various inflammatory cells, thereby potentially exacerbating inflammation. Additionally, the negative correlation with CCL3 and CCL5 suggests that PI3 may possess bidirectional immunoregulatory properties.

Our enrichment analysis suggests that the pathogenesis of both AD and UC may involve the JAK-STAT inflammatory pathway. Currently, upadacitinib, a JAK1 inhibitor, is approved for the treatment of moderate-to-severe AD and UC.[35,36] Recent studies have demonstrated that the JAK inhibitor ASN002 can reduce PI3 expression.[37] A previous study observing colitis mice treated with a PI3 transgenic drug found that increasing PI3 expression normalized the tight junction protein ZO-1 and modulated the intestinal flora.[38] In addition, PI3 promotes wound tissue repair and healing by inhibiting proteases and preventing extracellular matrix degradation.[39] Given its role in barrier repair and modulation of immune recruitment, PI3 may serve not only as a shared diagnostic biomarker for AD and UC but also as a potential therapeutic target—particularly for patients with poor responses to JAK inhibitors or severely compromised barriers.

Apart from this, our research revealed that 17 miRNAs (including has-miR-155, has-miR-21, and has-miR-223) and 2 transcription factors (YY1 and FOXP3) may be involved in the shared mechanisms of AD and UC. The role of FOXP3 in regulating the differentiation and function of CD4+ regulatory T cells (Tregs) to prevent immune hyperactivation and mediate immune suppression is well-established.[40,41] MiR-155 has been shown to play a crucial role in inflammation by targeting various genes that modulate Treg/Th17 immune balance, influencing both Foxp3 and RORγt expression.[42] The interaction between has-miR-155, FOXP3, and PI3 may represent a novel mechanism linking these two diseases. However, further studies are needed to validate the specific epigenetic mechanisms involved.

Nevertheless, there were some limitations to this study: Firstly, the primary aim of this study was to explore the association between AD and UC. However, both UC and CD were recognized as subtypes of IBD, and while they exhibited differing specificities, existing literature suggested that both conditions were linked to AD to varying extents. Additional scrutiny was warranted to elucidate these discrepancies. Secondly, in spite of a predicted epigenetic network of hub genes, more comprehensive empirical studies were required to investigate the downstream mechanisms of these genes.

Conclusion

In conclusion, our study provides a novel immunological perspective on the shared immune mechanisms of AD and UC. The high expression of PI3 in lesional tissues and its associations with immune cells and chemokines suggest that PI3 may serve as a common biomarker and potential therapeutic target for both diseases. The shared CCL and CXCL

signaling pathways indicate a common immune recruitment mechanism in AD and UC, offering a theoretical basis for developing dual-disease targeted therapeutic strategies.

Abbreviations

AUC, area under the curve of ROC; AD, atopic dermatitis; BP, biological processes; CD, crohn's disease; cDC1, conventional dendritic cell 1; DEGs, differentially expressed genes; DCs, dendritic cells; EPC, edge penetration component; GEO, gene expression omnibus; GO, gene ontology; GSEA, gene set enrichment analysis; HMDD, the human microRNA disease database; HC, healthy control; M, macrophages; IBD, inflammatory bowel disease; KEGG, kyoto encyclopedia of genes and genomes; KC, keratinocyte; LC, langerhans cell; LASSO, the least absolute shrinkage and selection operator; MNC, maximum neighborhood component; mDC, myeloid dendritic cell; pDC, plasmacytoid dendritic cell; PPI, protein–protein interaction; ROC, receiver operator characteristic; scRNA-seq, single-cell RNA sequencing; SVM-RFE, support vector machine - recursive feature elimination; TFs, transcription factors; UC, ulcerative colitis; UMAP, manifold approximation and projection; WGCNA, weighted gene co-expression network analysis.

Data Sharing Statement

All datasets used for analysis (GSE121212, GSE75214, GSE16161, GSE87466, GSE214695, GSE197023 and GSE153760) were derived from the Gene Expression Omnibus (GEO, https://www.ncbi.nlm.nih.gov/geo/) database, a publicly available dataset.

Ethics Approval

All experiments were approved by the Medical Ethics Committee of the Second Affiliated Hospital of Harbin Medical University (KY2018-030), and all participants have signed an informed consent form in accordance with the Declaration of Helsinki.

Acknowledgments

We acknowledged contributions from the GEO database and String database for sharing data and code.

Author Contributions

All authors made a significant contribution to the work reported, whether that is in the conception, study design, execution, acquisition of data, analysis and interpretation, or in all these areas; took part in drafting, revising or critically reviewing the article; gave final approval of the version to be published; have agreed on the journal to which the article has been submitted; and agree to be accountable for all aspects of the work. They guarantee that this article is the author's original work and has not been previously published or considered for publication elsewhere.

Funding

The project was supported by the National Natural Science Foundation of China (NSFC, Grant No. 82373477).

Disclosure

The authors declare no conflict of interest.

References

1. Weidinger S, Beck LA, Bieber T, Kabashima K, Irvine AD. Atopic dermatitis. *Nat Rev Dis Primers*. 2018;4(1):1. doi:10.1038/s41572-018-0001-z
2. Bylund S, Kobyletzki LB, Svalstedt M, Svensson Å. Prevalence and incidence of atopic dermatitis: a systematic review. *Acta Derm Venereol*. 2020;100(12):adv00160. doi:10.2340/00015555-3510
3. Schmitt J, Schwarz K, Baurecht H, et al. Atopic dermatitis is associated with an increased risk for rheumatoid arthritis and inflammatory bowel disease, and a decreased risk for type 1 diabetes. *J Allergy Clin Immunol*. 2016;137(1):130–136. doi:10.1016/j.jaci.2015.06.029
4. Ordás I, Eckmann L, Talamini M, Baumgart DC, Sandborn WJ. Ulcerative colitis. *Lancet*. 2012;380(9853):1606–1619. doi:10.1016/S0140-6736(12)60150-0
5. Kaplan GG. The global burden of IBD: from 2015 to 2025. *Nat Rev Gastroenterol Hepatol*. 2015;12(12):720–727. doi:10.1038/nrgastro.2015.150

6. Niwa Y, Sumi H, Akamatsu H. An association between ulcerative colitis and atopic dermatitis, diseases of impaired superficial barriers. *J Invest Dermatol*. 2004;123(5):999–1000. doi:10.1111/j.0022-202X.2004.23462.x
7. Lee H, Lee JH, Koh SJ, Park H. Bidirectional relationship between atopic dermatitis and inflammatory bowel disease: a systematic review and meta-analysis. *J Am Acad Dermatol*. 2020;83(5):1385–1394. doi:10.1016/j.jaad.2020.05.130
8. Shi X, Chen Q, Wang F. The bidirectional association between inflammatory bowel disease and atopic dermatitis: a systematic review and meta-analysis. *Dermatology*. 2020;236(6):546–553. doi:10.1159/000505290
9. Kim M, Choi KH, Hwang SW, Lee YB, Park HJ, Bae JM. Inflammatory bowel disease is associated with an increased risk of inflammatory skin diseases: a population-based cross-sectional study. *J Am Acad Dermatol*. 2017;76(1):40–48. doi:10.1016/j.jaad.2016.08.022
10. Kim KW, Koh SJ, Kang HW, et al. Atopic dermatitis is associated with the clinical course of inflammatory bowel disease. *Scand J Gastroenterol*. 2023;58(10):1115–1121. doi:10.1080/00365521.2023.2209688
11. Akdis CA. Does the epithelial barrier hypothesis explain the increase in allergy, autoimmunity and other chronic conditions? *Nat Rev Immunol*. 2021;21(11):739–751. doi:10.1038/s41577-021-00538-7
12. Zhu TH, Zhu TR, Tran KA, Sivamani RK, Shi VY. Epithelial barrier dysfunctions in atopic dermatitis: a skin-gut-lung model linking microbiome alteration and immune dysregulation. *Br J Dermatol*. 2018;179(3):570–581. doi:10.1111/bjd.16734
13. Cipriani F, Marzatico A, Ricci G. Autoimmune diseases involving skin and intestinal mucosa are more frequent in adolescents and young adults suffering from atopic dermatitis. *J Dermatol*. 2017;44(12):1341–1348. doi:10.1111/1346-8138.14031
14. O'Neill CA, Monteleone G, McLaughlin JT, Paus R. The gut-skin axis in health and disease: a paradigm with therapeutic implications. *Bioessays*. 2016;38(11):1167–1176. doi:10.1002/bies.201600008
15. Ellinghaus D, Baurecht H, Esparza-Gordillo J, et al. High-density genotyping study identifies four new susceptibility loci for atopic dermatitis. *Nat Genet*. 2013;45(7):808–812. doi:10.1038/ng.2642
16. Ritchie ME, Phipson B, Wu DI, et al. limma powers differential expression analyses for RNA-sequencing and microarray studies. *Nucleic Acids Res*. 2015;43(7):e47–e47. doi:10.1093/nar/gkv007
17. Yu G, Wang LG, Han Y, He QY. clusterProfiler: an R package for comparing biological themes among gene clusters. *OMICS*. 2012;16(5):284–287. doi:10.1089/omi.2011.0118
18. Thomas PD. The gene ontology and the meaning of biological function. *Methods Mol Biol*. 2017;1446:15–24. doi:10.1007/978-1-4939-3743-1_2
19. Kanehisa M, Goto S. KEGG: kyoto encyclopedia of genes and genomes. *Nucleic Acids Res*. 2000;28(1):27–30. doi:10.1093/nar/28.1.27
20. Kanehisa M, Furumichi M, Sato Y, Kawashima M, Ishiguro-Watanabe M. KEGG for taxonomy-based analysis of pathways and genomes. *Nucleic Acids Res*. 2023;51(D1):D587–D592. doi:10.1093/nar/gkac963
21. Kanehisa M. Toward understanding the origin and evolution of cellular organisms. *Protein Sci*. 2019;28(11):1947–1951. doi:10.1002/pro.3715
22. Langfelder P, Horvath S. WGCNA: an R package for weighted correlation network analysis. *BMC Bioinf*. 2008;9(1):559. doi:10.1186/1471-2105-9-559
23. Szklarczyk D, Gable AL, Lyon D, et al. STRING v11: protein-protein association networks with increased coverage, supporting functional discovery in genome-wide experimental datasets. *Nucleic Acids Res*. 2019;47(D1):D607–D613. doi:10.1093/nar/gky1131
24. Chin CH, Chen SH, Wu HH, Ho CW, Ko MT, Lin CY. cytoHubba: identifying hub objects and sub-networks from complex interactome. *BMC Syst Biol*. 2014;8 Suppl 4(Suppl 4):S11. doi:10.1186/1752-0509-8-S4-S11
25. Newman AM, Liu CL, Green MR, et al. Robust enumeration of cell subsets from tissue expression profiles. *Nat Methods*. 2015;12(5):453–457. doi:10.1038/nmeth.3337
26. Tibshirani R. Regression Shrinkage and Selection Via the Lasso. *J Royal Statistical Soc*. 1996;58(1):267–288. doi:10.1111/j.2517-6161.1996.tb02080.x
27. Breiman L. Random Forests. *Machine Learning*. 2001;45(1):5–32. doi:10.1023/A:1010933404324
28. Sanz H, Valim C, Vegas E, Oller JM, Reverter F. SVM-RFE: selection and visualization of the most relevant features through non-linear kernels. *BMC Bioinf*. 2018;19(1):432. doi:10.1186/s12859-018-2451-4
29. Huang Z, Shi J, Gao Y, et al. HMDD v3.0: a database for experimentally supported human microRNA-disease associations. *Nucleic Acids Res*. 2019;47(D1):D1013–D1017. doi:10.1093/nar/gky1010
30. Tong Z, Cui Q, Wang J, Zhou Y. TransmiR v2.0: an updated transcription factor-microRNA regulation database. *Nucleic Acids Res*. 2019;47(D1):D253–D258. doi:10.1093/nar/gky1023
31. Messeguer X, Escudero R, Farré D, Núñez O, Martínez J, Albà MM. PROMO: detection of known transcription regulatory elements using species-tailored searches. *Bioinformatics*. 2002;18(2):333–334. doi:10.1093/bioinformatics/18.2.333
32. James JP, Nielsen BS, Christensen IJ, et al. Mucosal expression of PI3, ANXA1, and VDR discriminates Crohn's disease from ulcerative colitis. *Sci Rep*. 2023;13(1):18421. doi:10.1038/s41598-023-45569-3
33. Brunner PM, Suárez-Fariñas M, He H, et al. The atopic dermatitis blood signature is characterized by increases in inflammatory and cardiovascular risk proteins. *Sci Rep*. 2017;7(1):8707. doi:10.1038/s41598-017-09207-z
34. Motta JP, Magne L, Descamps D, et al. Modifying the protease, antiprotease pattern by elafin overexpression protects mice from colitis. *Gastroenterology*. 2011;140(4):1272–1282. doi:10.1053/j.gastro.2010.12.050
35. Simpson EL, Papp KA, Blauvelt A, et al. Efficacy and safety of upadacitinib in patients with moderate to severe atopic dermatitis: analysis of follow-up data from the measure up 1 and measure up 2 randomized clinical trials. *JAMA Dermatol*. 2022;158(4):404–413. doi:10.1001/jamadermatol.2022.0029
36. Danese S, Vermeire S, Zhou W, et al. Upadacitinib as induction and maintenance therapy for moderately to severely active ulcerative colitis: results from three Phase 3, multicentre, double-blind, randomised trials. *Lancet*. 2022;399(10341):2113–2128. doi:10.1016/S0140-6736(22)00581-5
37. Pavel AB, Song T, Kim HJ, et al. Oral Janus kinase/SYK inhibition (ASN002) suppresses inflammation and improves epidermal barrier markers in patients with atopic dermatitis. *J Allergy Clin Immunol*. 2019;144(4):1011–1024. doi:10.1016/j.jaci.2019.07.013
38. Teng G, Liu Z, Liu Y, et al. Probiotic escherichia coli nissle 1917 expressing elafin protects against inflammation and restores the gut microbiota. *Front Microbiol*. 2022;13:819336. doi:10.3389/fmicb.2022.819336
39. Deraison C, Bonnart C, Langella P, Roget K, Vergnolle N. Elafin and its precursor trappin-2: what is their therapeutic potential for intestinal diseases? *Br J Pharmacol*. 2023;180(2):144–160. doi:10.1111/bph.15985

40. Shu Y, Hu Q, Long H, Chang C, Lu Q, Xiao R. Epigenetic variability of CD4+CD25+ tregs contributes to the pathogenesis of autoimmune diseases. *Clin Rev Allergy Immunol*. 2017;52(2):260–272. doi:10.1007/s12016-016-8590-3
41. Barbi J, Pardoll D, Pan F. Treg functional stability and its responsiveness to the microenvironment. *Immunol Rev*. 2014;259(1):115–139. doi:10.1111/imr.12172
42. Hu J, Huang S, Liu X, Zhang Y, Wei S, Hu X. miR-155: an important role in inflammation response. *J Immunol Res*. 2022;2022:7437281. doi:10.1155/2022/7437281